Nano Research

ISSN 1998-0124 CN 11-5974/O4
https://doi.org/10.1007/s12274-022-5060-5

Review Article

Single-atom nanozymes: From bench to bedside

Chanyuan Jin[1], Sanjun Fan[2], Zechao Zhuang[3] (✉), and Yongsheng Zhou[4] (✉)

[1] *Second Dental Center, Peking University School and Hospital of Stomatology, Beijing 100101, China*
[2] *Department of Chemistry and Biochemistry, The Ohio State University, Columbus, OH 43210, USA*
[3] *Department of Chemistry, Tsinghua University, Beijing 100084, China*
[4] *Department of Prosthodontics, Peking University School and Hospital of Stomatology & National Center of Stomatology & National Clinical Research Center for Oral Diseases & National Engineering Research Center of Oral Biomaterials and Digital Medical Devices & Beijing Key Laboratory of Digital Stomatology, Beijing 100081, China*

Received: 7 August 2022 / **Revised:** 12 September 2022 / **Accepted:** 14 September 2022

ABSTRACT

Single-atom nanozymes (SANs) are the new emerging catalytic nanomaterials with enzyme-mimetic activities, which have many extraordinary merits, such as low-cost preparation, maximum atom utilization, ideal catalytic activity, and optimized selectivity. With these advantages, SANs have received extensive research attention in the fields of chemistry, energy conversion, and environmental purification. Recently, a growing number of studies have shown the great promise of SANs in biological applications. In this article, we present the most recent developments of SANs in anti-infective treatment, cancer diagnosis and therapy, biosensing, and antioxidative therapy. This text is expected to better guide the readers to understand the current state and future clinical possibilities of SANs in medical applications.

KEYWORDS

single-atom nanozymes, cancer therapy, biosensing, anti-infective treatment, antioxidative therapy

1 Introduction

Enzymes are catalytically active proteins or RNAs produced by cells which speed up specific biological reactions in living organisms. They have an enormous potential for being applied in various fields like environmental protection, biomedicine, agricultural engineering, and food industry [1–3]. However, the protein or RNA nature of enzymes hinders their large-scale application because of their instability, high preparation cost, immunogenicity, low recycling efficiency, and strict requirements for external conditions. Thus, it is meaningful to develop various artificial catalysts for different reactions [4–7]. Benefiting from the progress of nanotechnology, more and more nanomaterial-based enzyme mimics have been discovered [8, 9]. In 2004, the name "nanozyme" was firstly proposed by Scrimin, describing a gold nanoparticle-based transphosphorylation catalyst [10]. Three years later, Yan et al. found that Fe_3O_4 nanoparticles have peroxidase (POD)-like activities, which significantly encouraged the development of nanozymes [11]. Nanozymes have attracted worldwide attention due to their advantages of low cost, convenient preparation, long-term storage, less immunogenicity, and especially higher efficiency [9, 12–14]. Nonetheless, the practical application of nanozymes is constrained by their ambiguous structure, uncertain catalytic mechanism, and insufficient substrate selectivity.

With the progress of synthetic technologies, in 2011, Zhang et al. firstly brought the term of "single-atom catalysts (SACs)" and opened a new window for nanozymes by fabricating a novel single-atom Pt_1/FeO_x catalyst, which possessed high catalytic activity for CO oxidation [15]. Subsequently, numerous researchers have devoted themselves to synthesizing more variety of SACs [16–22]. Up to now, various kinds of SACs including noble metal-based SACs (e.g., Au, Pd, Pt, and Ag), common metal-based SACs (e.g., Fe, Co, Ni, Cu, and Zn), and dual metal SACs exhibiting excellent performance have been successfully prepared for diverse catalytic reactions [23–25]. SACs combine the strong points of homogeneous and heterogeneous catalysts and exhibit superiority in catalytic activity and selectivity. Undoubtedly, SACs have become a research hotspot and frontier trend in the field of energy storage and conversion, electrocatalysis, thermocatalysis, photocatalysis, etc. [26–35]. In contrast with the conventional metal catalysts, SACs are formulated by uniformly isolating separate single metal atoms onto various supports. SACs have diverse types of structures, such as M-N_x (M: Fe, Mn, Co, Zn, Cu, etc.; N: nitrogen), metal-metal oxides (e.g., Pt/CeO_2) [21]. Among SACs, M-N_x SACs have been intensively studied and are expected to be substitutes for natural enzymes because the stable coordination bonds (M–N_x) formed between metal atoms and nitrogen atoms are similar to natural metalloenzymes, such as heme Fe–N_4 and cytochrome P450. Since the structure and catalytic performance of SACs can be fabricated similar to natural enzymes, SACs with enzyme-like properties can be used for mimicking the biocatalytic reactions and referred to as single-atom nanozymes (SANs) [36, 37]. Attributed to their superior performance, high substrate specificities, excellent catalytic activity, and good biocompatibility, single-atom catalysts exhibit huge application potential in biomedicine [38–40]. In this review, we mainly focus on the latest research progress of single-atom

Address correspondence to Yongsheng Zhou, kqzhouysh@hsc.pku.edu.cn; Zechao Zhuang, zhuangzc@mail.tsinghua.edu.cn

nanozymes in biomedical applications, including anti-infective treatment, cancer diagnosis and treatment, biosensing, and antioxidative therapy.

2 Applications of SANs in the treatment of infection

Infectious diseases caused by bacteria or virus pose a huge threat to health and even lead to death. Infection can occur in almost all organs or systems of the body. In recent decades, antibiotics have been considered as terminators of infections. However, the misuse and abuse of antibiotics results in the emergence of drug-resistant bacteria. It is estimated 700,000 people a year die of drug-resistant bacteria infections [41–43]. In this case, it is important to develop novel materials for treating infections [44, 45]. Recently, SACs/SANs have shown great potential in fighting against the infection (Table 1).

Table 1 Applications of SACs/SANs in infection treatment

SACs/SANs	Enzyme-like activities	Application	References
g-ZnN_4-MoS_2	Sonocatalytic property	Osteomyelitis treatment	[46]
HNTM-Pt@Au	Sonocatalytic property	Osteomyelitis treatment	[47]
Cu SASs/NPC	POD, GSH	Wound disinfection	[48]
PMCSs	POD	Wound disinfection	[49]
SAF NCs	POD	Wound disinfection	[50]
FeN_5 SA/CNF	OXD	Wound disinfection	[51]
Co/PMCS	SOD, CAT, GSH-Px	Sepsis	[52]
Ag-TiO_2	POD	Elimination of SARS-CoV2	[53]

2.1 Treatment of bone infection

Bone infection is mainly caused by bacteria and can lead to progressive bone destruction, permanent disability, and even death. Despite current treatment combines various antibiotics with surgery, the emergence of multi-drug resistant microbes presents significant therapeutic challenges [54, 55]. Recent studies have demonstrated SACs provide a new breakthrough for the treatment of osteomyelitis. For example, Feng and co-workers designed a sonosensitizer named g-ZnN_4-MoS_2, consisting of porphyrin-like Zn single-atom catalysts (g-ZnN_4) and MoS_2 quantum dots [46]. The antibacterial efficiency of killing methicillin-resistant *Staphylococcus aureus* (MRSA) could reach 99.58% via efficiently generating O_2 under ultrasound irradiation. Moreover, the sustained release of Zn^{2+} from g-ZnN_4-MoS_2 in safe concentration significantly promoted osteogenic differentiation (Fig. 1(a)).

In another study, Yu and colleagues fabricated a single-atom catalyst consisting of rat red cell membrane (RBC) and gold nanorods (Au NRs) driving single-atom doping zirconium-based porphyrin metal-organic skeleton (HNTM-Pt@Au). The obtained RBC-HNTM-Pt@Au showed good efficacy in treating osteomyelitis caused by MRSA via its sonodynamic bactericidal activity and dynamic detoxification ability (Fig. 1(b)). The above works suggested that SACs could be therapeutic alternatives for efficient treatment of bone infection [47].

2.2 Treatment of infected wounds

Wound infection is one of the leading causes of non-healing wounds [56, 57]. Recent studies showed SANs could accelerate the wound healing process. For example, Cu single-atom sites/N

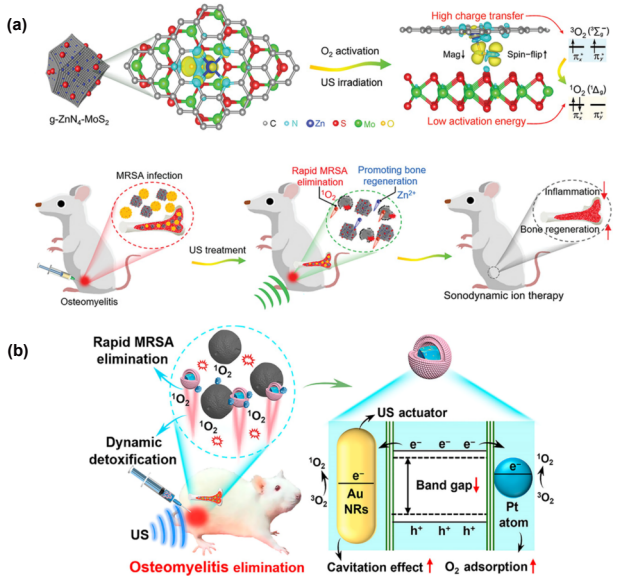

Figure 1 Application of single-atom catalysts in bone infection treatment. (a) Schematic illustration of treatment of osteomyelitis through g-ZnN_4-MoS_2. Reproduced with permission from Ref. [46], © Feng, X. B. et al. 2021. (b) Schematic illustration of treatment of osteomyelitis through RBC-HNTM-Pt@Au. Reproduced with permission from Ref. [47], © American Chemical Society 2021.

doped porous carbon (Cu SASs/NPC) was produced through a pyrolysis-etching-adsorption-pyrolysis method [48], which exhibited higher POD-like catalytic activity and generated a great amount of hydroxyl radicals (·OH) to fight bacteria. In addition, the glutathione peroxidase (GSH-Px)-mimic property of Cu SASs/NPC also assists the sterilization effect by depleting GSH of bacteria. Moreover, the noteworthy near-infrared light absorption ability of Cu SASs/NPC generated hyperthermia and improved the POD-like catalytic activity to kill bacteria. The MRSA-infected wound model revealed that Cu SASs/NPC could remarkably eliminate bacterial infections and promote wound healing (Fig. 2(a)). Xu and coworkers prepared a SAN by using zinc-based zeolitic-imidazolate framework (ZIF-8) as precursor. This SAN (named PMCSs) showed excellent POD-like activity, which could effectively inhibit *Pseudomonas aeruginosa* and eventually significantly accelerate wound healing [49].

Huo et al. prepared a nitrogen-doped amorphous carbon supported iron single-atom Fe nanocatalysts (SAF NCs) with POD-mimic activities and excellent photothermal performance [50]. Both the Gram-negative representative bacteria *Escherichia coli* and Gram-positive representative bacteria *S. aureus* could be effectively killed at 62.5 μg/mL of SAF NCs. Moreover, the antibacterial efficiency was enhanced by the photothermal performance of SAF NCs. Bacterial infection models proved that SAF NCs effectively eradicated *E. coli* and *S. aureus* and aided wound healing (Fig. 2(b)). Huang and fellows developed a SAN of axial N-coordinated single-atom Fe confined by carbon nanoframe (FeN_5 SA/CNF) via bottom-up strategy [51]. They found FeN_5 SA/CNF exhibited excellent bactericidal effect and promoted wound healing *in vivo*.

2.3 Treatment of sepsis

Sepsis, which has high morbidity and mortality, is a severe organ dysfunction resulted from the dysregulated host response to infection [58, 59]. During sepsis, overproduction of endogenous reactive oxygen species (ROS) and reactive nitrogen species (RNS) results in cytotoxic effects and organ damage [60, 61]. It is urgent to develop new materials with the ability to obliterate ROS and RNS. In 2020, Cao et al. prepared Co/PMCS through the high

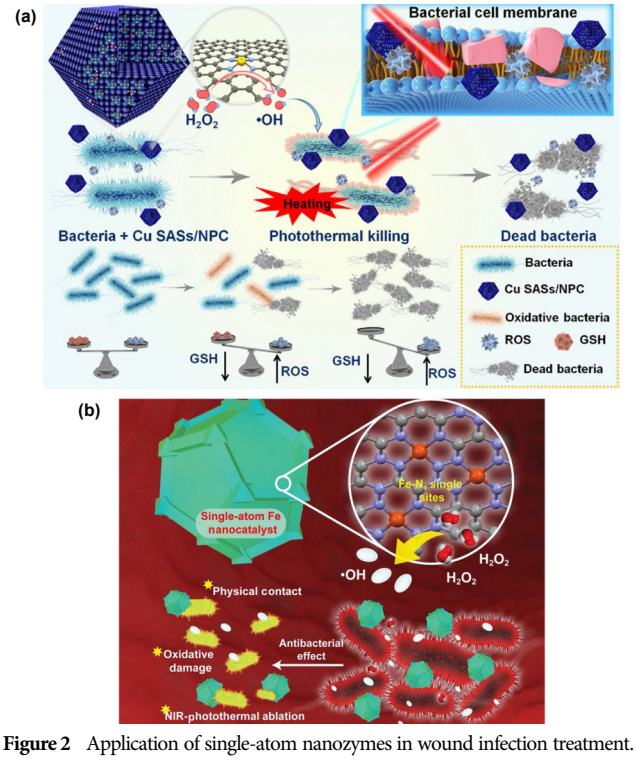

Figure 2 Application of single-atom nanozymes in wound infection treatment. (a) Cu SASs/NPC were prepared against bacteria. Reproduced with permission from Ref. [48], © Wang, X. W. et al. 2021. (b) Antibacterial effect of SAF NCs. Reproduced with permission from Ref. [50], © WILEY-VCH Verlag GmbH & Co. KGaA, Weinheim 2019.

temperature decomposition of Co-doped ZIF-8, which could efficiently scavenge multiple ROS and RNS to mitigate sepsis [52]. Co/PMCS possessed excellent superoxide dismutase (SOD)-like activity, catalase (CAT)-like activity, and GSH-Px-like activity to eliminate O_2^- and hydrogen peroxide (H_2O_2) and removed ·OH through the redox cycling. More importantly, Co/PMCS also eliminated nitric oxide by forming nitrosyl-metal complex. *In vivo* lipopolysaccharide (LPS)-induced sepsis model showed Co-SACs could not only effectively reduce pro-inflammatory cytokines, but also reduce the production of systemic ROS and RNS and promote functional recovery of multiple organs in mice with sepsis. This study proved the therapeutic potentials of SANs for sepsis management.

2.4 Antiviral activity against coronavirus

The emergence of severe acute respiratory syndrome coronavirus 2 (SARS-CoV2) has caused an unprecedented pandemic, which not only threatens human health, but also drastically affects our way of life and puts a huge burden on the economy of entire world [62]. Up to date, there are no specific drugs against SARS-CoV2. Recently, Wang et al. prepared a titanium dioxide supported SAN composed of atomically dispersed silver atoms (Ag-TiO_2 SAN) using a wet chemistry technology [53]. Since Ag-TiO_2 SAN can interact with the spike protein of SARS-CoV2, the adsorption capacity of Ag-TiO_2 SAN to pseudo-typed SARS-CoV2 was higher than that of traditional nano-Ag and nano-TiO_2. Besides, the strong binding between Ag atoms of Ag-TiO_2 SAN and cysteine and asparagine of spike 1 receptor binding domain (S1 RBD) significantly inhibited the binding of S1 RBD to human angiotensin converting enzyme 2 and thus protected host cells against SARS-CoV2 infection.

Ag-TiO_2 SAN promoted the ingestion of pseudo-typed SARS-CoV2 by macrophages, and subsequently induced high level of ROS in macrophages lysosomes under acid conditions, thereby degrading the virus without damaging cells. *In vivo* experiment indicated that Ag-TiO_2 SAN exhibited efficient antiviral activity against pseudo-typed SARS-CoV2 in the early and late infection phases (Fig. 3). These results prompted us to design more SANs against SARS-CoV2.

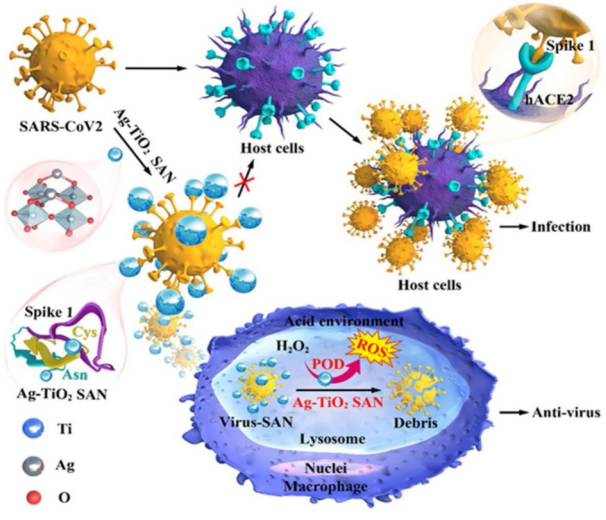

Figure 3 Schematic illustration of the anti-SARS-CoV2 activity of Ag-TiO_2 SAN. Reproduced with permission from Ref. [53], © Wang, D. J. et al. 2021.

3 Applications of SANs in cancer diagnosis and therapy

Cancer is one of the most feared disabling diseases, which is difficult to be diagnosed at early stage and has a high mortality. It brings both physical and mental damage to individuals and imposes huge economic burden on the family and society. Despite significant advances in theories and technologies of surgery therapy, chemotherapy, and radiotherapy, these conventional methods encounter many problems and challenges such as high cost, low therapeutic efficiencies, drug resistance, and undesirable severe side effects. Hence, it is of great significance to find more effective ways to diagnose and treat cancer. In the last decades, multiple studies demonstrated the great potential of SACs/SANs in cancer diagnosis and treatment (Table 2). SACs/SANs can be used in combination with other therapeutic patterns, which could remarkably enhance the anticancer efficacy while reduce the side effects [63–70].

3.1 Diagnosis of prostate cancer

Prostate cancer is a common malignant cancer in male worldwide [84]. The early diagnosis of cancer is critical for the therapeutic efficacy and prognosis. The screening and diagnosis of prostate cancer often relies on the measurement of prostate specific antigen (PSA), which is generated from prostatic epithelial cells and elevated in prostate cancer and other prostate diseases [85, 86].

Based on ion exchange reaction of $Zn_{0.5}Cd_{0.5}S$ anchored by single-atom Pt (denoted as Pt SA-$Zn_{0.5}Cd_{0.5}S$) with cupric oxide nanoparticle, a highly sensitive photoelectrochemical immunoassay was successfully constructed for determination of PSA [71]. Pt SA-$Zn_{0.5}Cd_{0.5}S$ exhibited strong specificity and ultra-sensitivity for PSA and the detection limit was as low as 0.22 pg/mL. There is not much difference between commercialized PSA ELISA kit and Pt SA-$Zn_{0.5}Cd_{0.5}S$ in determination of PSA, suggesting Pt SA-$Zn_{0.5}Cd_{0.5}S$ has great potential for prostate cancer screening and diagnosis.

In another study, Chen et al. synthesized a Pt clusters loaded Fe single-atom catalyst (denoted as Fe_{SA}-Pt_C) [72]. Owing to the hierarchical porous structure and synergism of Fe single-atom and

Table 2 Applications of SACs/SANs in cancer diagnosis and treatment

SACs/SANs	Enzyme-like activities	Application	References
Pt SA-$Zn_{0.5}Cd_{0.5}S$	Photocatalyst	Detection of PSA	[71]
Fe_{SA}-Pt_C	POD	Detection of PSA	[72]
Ru SAN	OXD, POD, GSHOx	Breast cancer treatment	[73]
OxgeMCC-r	CAT	Breast cancer treatment	[74]
FeN_5	POD	Breast cancer treatment	[75]
Mn/PSAE	CAT, OXD, POD	Breast cancer treatment	[76]
Pd SAN	POD, GSHOx	Breast cancer treatment	[77]
PMS	POD	Breast cancer treatment	[78]
SAFe-NMCNs	CAT, POD	Breast cancer treatment	[79]
SAF NPs@DOX@CM	POD	Lung cancer treatment	[80]
Au-Fe SAN	GOD	Esophageal cancer treatment	[81]
Fe SAN	Fenton-like, OXD, POD	Osteosarcoma treatment	[82]
MitoCAT-g	OXD	Liver cancer treatment	[83]

Pt clusters, Fe_{SA}-Pt_C possessed highly active POD-like activity. The cascade signal amplification method was constructed for detection of PSA by combining glucose oxidase (GOD) with POD-like Fe_{SA}-Pt_C nanozyme, exhibiting a wide linearity range of PSA (8 to 1,000 pg/mL) and a low detection limit at 1.8 pg/mL.

3.2 Breast cancer treatment

According to the recent statistics of the International Agency for Research on Cancer, breast cancer has become the most diagnosed cancer in both sexes [87]. Much attention has been paid to develop novel materials for breast cancer treatment [88–91]. Recently, increasing number of studies have shown the efficiency of single-atom nanozymes in breast cancer therapy. For instance, Wang et al. prepared Ru SAN by loading dispersed Ru single-atoms on biocompatible carbon dot via a pyrolyzing coordinated complex strategy [73]. Ru SAN exhibited various enzyme-like activities, including oxidase (OXD)-like activity, POD-like activity, and glutathione oxidase (GSHOx)-like activity, which produced ROS and depleted glutathione simultaneously, thus inducing intracellular oxidative damage and ultimately resulting in breast cancer cells death. Moreover, the excellent photothermal stability of Ru SAN improved the therapeutic effect. *In vivo* assay showed the tumors remarkably disappeared on day 8 in Ru SAN group after the addition of laser (Fig. 4(a)). Another research group prepared a SAN (denoted as OxgeMCC-r) by isolating single-atom ruthenium on a metal-organic skeleton $Mn_3[Co(CN)_6]_2$ with photosensitizer chlorin e6 (Ce6) [74]. The results showed that the obtained OxgeMCC-r SAN effectively enhanced ROS generation, enhanced photodynamic therapy (PDT) efficiency, and killed nearly 90% of breast cancer cells.

Xu et al. synthesized an iron-based SAN containing five-coordinated structure (FeN_5) which could effectively kill breast cancer cells by the oxidative damage of ROS due to the excellent POD-like activity [75]. Zhu et al. reported a manganese-based PEGylated SAN (Mn/PSAE) could effectively generate abundant toxic ROS [76]. In addition to mimicking the multiple catalytic activity of CAT, OXD, and POD enzymes, Mn/PSAE also possessed excellent photothermal performance. The authors confirmed the enzymatic and photothermal activities of Mn/PSAE synergistically killing breast cancer cells.

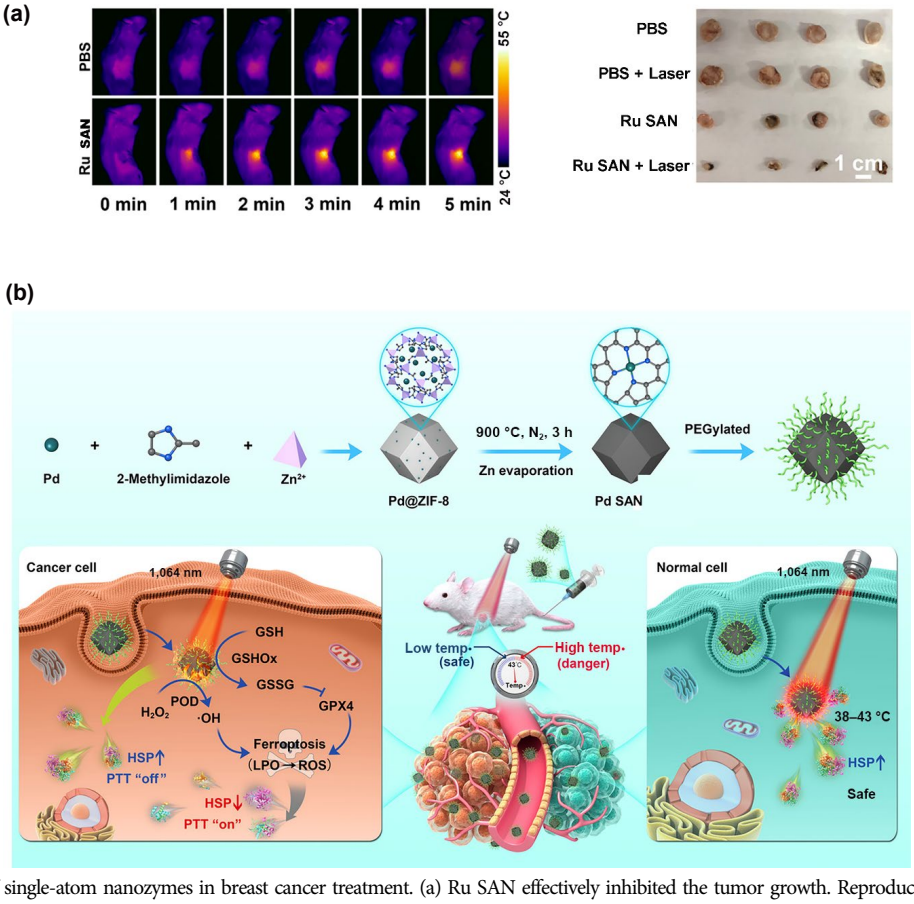

Figure 4 Application of single-atom nanozymes in breast cancer treatment. (a) Ru SAN effectively inhibited the tumor growth. Reproduced with permission from Ref. [73], © American Chemical Society 2021. (b) The synthesis of PEGylated Pd SAN and the mechanism by which mild PTT promoted ferroptosis. Reproduced with permission from Ref. [77], © Wiley-VCH GmbH 2021.

Nanoparticle-based photothermal therapy (PTT) is a prospective strategy for cancer treatment, which converts laser energy into heat to destroy cancer cells. However, the PTT efficacy is alleviated once cancer cells expressed heat-shock proteins. Moreover, PTT brings excessive heat which inevitably damages the proximal tissues. Thus, it is imperative to develop a low-temperature PTT strategy with higher efficiency and minimal harm to adjacent tissues at the same time. Chang et al. prepared a Pd SAN with POD and GSHOx mimic activities and photothermal conversion performance [77]. Pd SAN upregulated the amount of ROS and lipid peroxides and thus inhibited the expression of heat shock proteins and finally enabled mild PTT. Chang et al. demonstrated Pd SAN could successfully make breast cancer cells sensitive to mild PTT with high curative effect and good biosafety (Fig. 4(b)). Qi et al. also developed a low-temperature PTT strategy by formulating a platelet membrane-coated mesoporous Fe SAN (PMS) [78]. The obtained PMS showed a high POD activity, good photothermal property, and excellent tumor-targeting ability, which may also be applied as drugs carrier. Results showed that PMS could enhance mild-temperature PTT efficacy and inhibited growth of breast cancer cells with minimal injury to normal tissues at the same time. In another study, Su et al. designed a dual enzyme mimic single-atom Fe dispersed N-doped mesoporous carbon nanospheres nanozyme (denoted as SAFe-NMCNs) possessing remarkable light-to-heat conversion capability, which could efficiently suppress growth of breast cancer cells through a synergistic therapeutic effect with photothermal-enhanced nano-catalytic treatment [79].

3.3 Lung cancer treatment

The mortality of lung cancer is highest among all cancer types, which has attracted widespread attention from researchers [92]. Recently, Liu et al. prepared single-atom Fe-containing nanoparticles (SAF NPs) for killing lung cancer cells. SAF NPs possessed POD-like activity, which could produce plenty of toxic ·OH and consequently have a significant antitumor effect [80]. Moreover, antitumor drug doxorubicin (DOX) was effectively delivered by SAF NPs owing to the porous structure. Since cancer cell membrane (CM) has attract extensive attention in cancer therapy, Liu et al. camouflaged SAF NPs with lung cancer cell (A549) membrane, which improved the biological compatibility, prolonged blood circulation time, helped SAF NPs escaped from early systemic clearance, and increased tumor targeting. *In vivo* BALB/c nude mice experiments showed SAF NPs + DOX + A549 CM group exhibited the most significant tumor suppressive effect (Fig. 5).

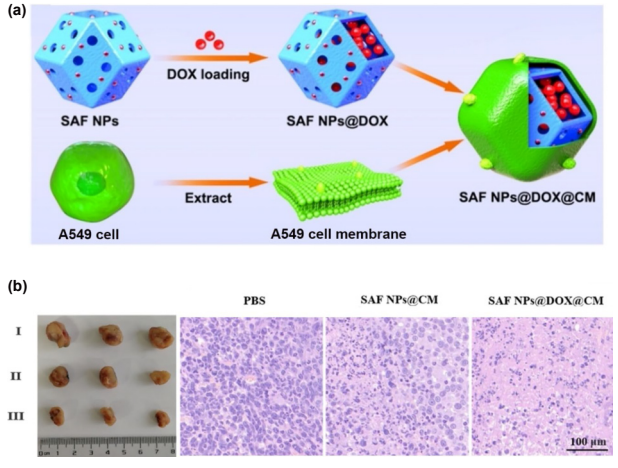

Figure 5 Application of single-atom nanozyme in lung cancer treatment. (a) The synthesis of SAF NPs@DOX@CM. (b) SAF NPs@DOX@CM showed the most obvious tumor suppressive effect. Reproduced with permission from Ref. [80], © Wiley-VCH GmbH 2021.

3.4 Esophageal cancer treatment

The high malignancy and poor survival rate of esophageal cancer highlight the need for developing new treatment strategies [93, 94]. Feng et al. established Au-FeSAN through the fixation of an ultra-small Au nanozyme into a metal-organic skeleton [81]. Owing to the interaction between Au nanoparticles with glucose, this SAN exhibited excellent GOD-like activity, which could reduce the intracellular glucose level of tumor cells, inhibit the expression of HSP, and realize low temperature PTT. The Au-FeSAN exhibited satisfactory photodynamic and photothermal performances and POD activity, enabling simultaneous efficient chemodynamic, photothermal, and photodynamic tumor therapy under near-infrared light. *In vivo* esophagus cancer model revealed that the Au-FeSAN group exhibited remarkably higher tumor inhibition rate without any substantial side effects.

3.5 Osteosarcoma treatment

In a recent study, a SAN for the treatment of osteosarcoma was successfully developed by dispersing single-atom Fe catalysts (FeSAN) onto a three-dimensional (3D) printed bioactive glass (BG) scaffold [82]. The authors demonstrated that the FeSAN composite scaffold effectively eliminated both osteosarcoma cells and bacteria. Mechanistically, they found FeSAN displayed superior Fenton catalytic activity to produce large quantities of toxic ·OH. Moreover, FeSAN exhibited OXD-like and POD-like activities and favorable photothermal effect to kill osteosarcoma cells and bacteria. Besides, *in vivo* experiments showed that the BG scaffold promoted the osteogenesis of bone marrow derived mesenchymal stem cells in the bone defects. The combination of Fe SAN with BG scaffold exhibited antibacterial, anti-tumor, and osteo-inductive effects simultaneously, advancing the application of SAN in osteosarcoma treatment (Fig. 6).

3.6 Liver cancer treatment

Another study developed a promising agent (MitoCAT-g) for liver cancer treatment, which consists of atomically dispersed gold supported by carbon-dot (CAT-g) with modifications of ROS-producing cinnamaldehyde and mitochondrion-targeting triphenylphosphine. The endocytosis of MitoCAT-g leads to the amplification of oxidative stress in mitochondria via depleting antioxidant GSH and elevating ROS, ultimately leading to the highest degree of cancer cell apoptosis. Meanwhile, MitoCAT-g showed limited cytotoxicity to normal cells because of the lower level of oxidative stress in normal cells [83]. *In vivo* experiments demonstrated that MitoCAT-g significantly inhibited tumor growth.

4 Applications of SANs in biosensing

Although various nanozymes with OXD, POD, or other enzyme-like activities have been applied in biosensing, the lower catalytic activity and unsatisfactory selectivity hinder the application. Owing to the excellent catalytic activity and substrate selectivity of SANs, there has been a boom in the usage of SANs in biosensing [95–103]. SANs have been conducted to detect various types of biomolecules, such as small molecules and proteins (Table 3).

4.1 Acetylcholine and acetylcholinesterase

Wu et al. synthesized Cu-N-C SAN using a salt-template method, which exhibited POD-like activity [104]. The authors established three-enzyme cascade system consisting of acetylcholinesterase, choline oxidase, and Cu-N-C SAN for tracing the amounts of

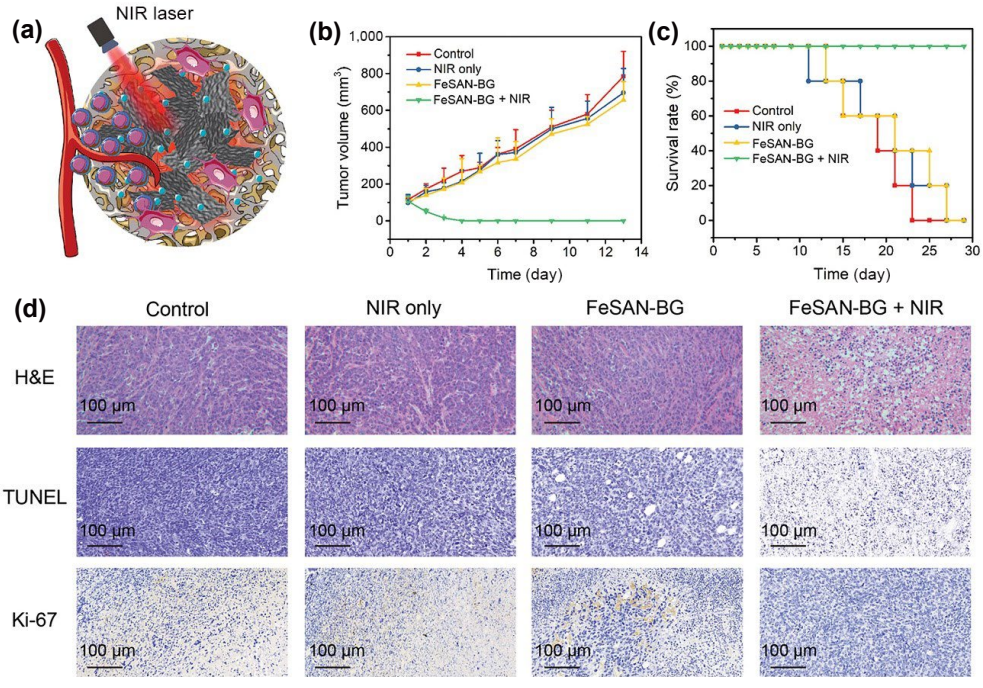

Figure 6 Application of single-atom nanozyme in osteosarcoma treatment. (a) Illustration of osteosarcoma ablation achieved by FeSAN-BG. (b) Tumor volume and (c) survival rates of mice in each group. Control: saline; and near-infrared (NIR) only: primitive BG scaffold + NIR. (d) Hematoxylin and eosin (H&E) staining, terminal deoxynucleotidyl transferase-mediated dUTP nick end labeling (TUNEL) staining, and antigen Ki-67 staining showed that FeSAN-BG + NIR effectively eliminated tumor tissue. Scale bar: 100 μm. Reproduced with permission from Ref. [82], © Wiley-VCH GmbH 2021.

Table 3 Applications of SACs/SANs in biosensing

SACs/SANs	Enzyme-like activities	Detection	References
Cu-N-C	POD	Acetylcholine	[104]
Fe-N-C	OXD	Acetylcholinesterase	[105]
Fe SAN	POD	Acetylcholinesterase	[106]
Fe-N-C	POD	Butyryl cholinesterase	[107]
Fe/NC-SAN	POD	Alkaline phosphatase	[108]
Fe-N/C	OXD	Alkaline phosphatase	[109]
CNT/FeNC	POD	Glucose, ascorbic acid, H_2O_2	[110]
Co-SAC	Electrocatalytic property	Glucose	[111]
Fe SSN	POD	Glucose	[112]
Fe-N/C-CNT	OXD	GSH	[113]
Fe-NDs	POD, OXD	GSH, H_2O_2	[114]
Fe-N-C SAN	POD	H_2O_2	[115]

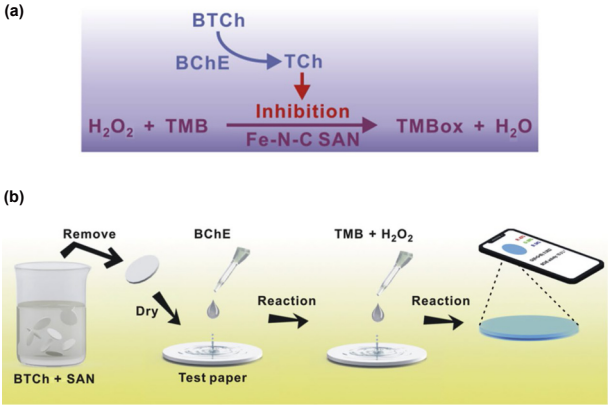

Figure 7 Application of single-atom nanozyme in the detection of BChE activity. (a) Illustration of the biosensing principle of BChE activity. BTch: S-butyrylthiocholine iodide. (b) Illustration of the paper bioassay procedure for BChE activity. Reproduced with permission from Ref. [107], © Elsevier B.V. 2019.

acetylcholine. This study showed the ascendancy of Cu-based SAN with plentiful active sites in biosensing.

Since mercapto molecules could interact with Fe-N-C single-atom nanozyme (Fe-N-C SAN) and suppress the nanozyme activity, Wu and colleagues developed Fe-N-C SAN based biosensor for detection of the acetylcholinesterase activity [105]. In another study, Qin et al. also constructed photoelectrochemical sensing platform for detection of acetylcholinesterase activity via harnessing the oxygen reduction property and POD-like activity of Fe SAN [106].

4.2 Butyryl cholinesterase

Niu et al. proposed a Fe-N-C SAN for replacing natural horseradish peroxidase (HRP) to detect butyrylcholinesterase (BChE) activity, which exhibited unprecedented POD-mimicking activity (Fig. 7). Due to the 100% active iron sites utilization and the porous carbon support with large surface area, the specific activity of Fe-N-C SAN was as high as 57.76 U/mg, which was far superior to other POD mimics and close to that of natural HRP [107]. Notably, the Fe-N-C SAN exhibited excellent storage stability and favorable robustness under harsh conditions, indicating its potential to act as candidate of natural HRP in biosensing application.

4.3 Alkaline phosphatase

Xie and coworkers established Fe-N-C single-atom nanozyme (Fe/NC-SAN) for detection of alkaline phosphatase (ALP) activity [108]. Fe/NC-SAN possessing excellent POD-like activity could oxidize 3,3′5,5′-tetramethylbenzidine (TMB) to a blue color, and the blue color faded after adding ascorbic acid. ALP could catalyze ascorbic acid 2-phosphate to generate ascorbic acid. Results showed that Fe/NC-SAN provided a detection limit (0.05 U/L) with high selectivity, anti-interference, and good stability. The practicability of Fe/NC-SAN-based assay was verified by serum samples from human, suggesting Fe/NC-SAN could be used as

alternative for detecting ALP in clinical application. In another study, a Fe-N/C nanozyme based biosensing strategy was designed for screening ALP activity, which possessed a detection scope of 0.05 to 100 U/L and minimum concentration limit of 0.02 U/L [109].

4.4 Glucose and ascorbic acid

Cheng et al. proposed a novel SAN (CNT/FeNC) with excellent POD-like activity, enabling ultrasensitive quantitation of ascorbic acid, glucose, and H_2O_2. The catalytic capacity parameter of CNT/FeNC was 4,500 times more than that of the classical Fe_3O_4 nanozyme [110]. Hou et al. established an online electrochemical biosensor using Co single-atom catalyst for *in vivo* monitoring of glucose [111].

In another study, single iron site nanozyme (Fe SSN) was prepared for quantification of glucose via a support-sacrificed strategy. The Fe SSN exhibited high POD activity and successfully catalyzed TMB into oxidized TMB with color change [112]. Based on Fe SSN, the authors established a low cost and ultrasensitive colorimetric platform for visual assessment and rapid quantitative determination of glucose, which is better than most reported colorimetric glucose assays (Fig. 8).

4.5 GSH

GSH is critical for maintaining redox homeostasis. It is of great significance to develop methods for GSH detection [116]. Wang and coworkers proposed an Fe-N/C-CNT nanomaterial, which showed splendid OXD-mimicking activity and was further used as viable colorimetric biosensor for detecting GSH [113]. In another study, Liu et al designed single-atom iron oxide nanoparticle-modified nanodiamonds (Fe-NDs), which exhibited POD-like and OXD-like activities. Fe-NDs could oxidize TMB from colorless to blue color, while adding GSH could reduce blue-colored oxidized TMB to colorless TMB. Hence, the Fe-NDs based biosensor for detecting GSH was established by measuring the absorbance. The results showed that the Fe-NDs-based sensor has a lower detection limit compared to the previously reported nanozyme-based colorimetric GSH sensors [114].

4.6 H_2O_2

Recently, detection of H_2O_2 has attracted much attention from researchers [117]. Jiao et al. prepared Fe-N-C SAN by using one pot calcination at high temperature, which exhibited POD-like activity. Attributed to the maximum atomic utilization, Fe-N-C SAN exhibited higher catalytic efficiency than other POD-like nanozymes. *In vitro* experiment proved the satisfactory sensitivity and specificity of Fe-N-C SAN for the quantitative determination of H_2O_2. For practical applications, the authors also performed a quantitative determination of H_2O_2 produced from the Hela cells with Fe-N-C SAN [115].

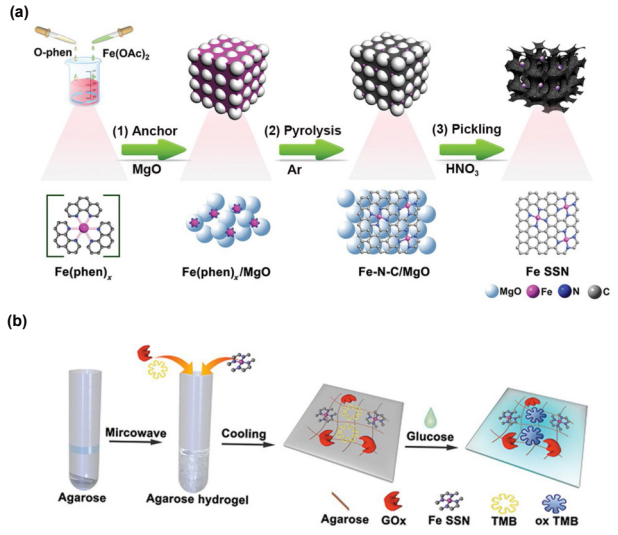

Figure 8 Application of single-atom nanozyme in the detection of glucose. (a) The synthesis of Fe SSN. (b) Illustration of agarose-based hydrogel colorimetric quantification of glucose. Reproduced with permission from Ref. [112], © WILEY-VCH Verlag GmbH & Co. KGaA, Weinheim 2020.

5 Applications of SANs in antioxidative therapy

Owing to the multi-antioxidant activities, SANs were also used for cyto-protection [118, 119]. For example, Ma et al. prepared a bifunctional Fe-SAs/NC catalysts with excellent CAT-like and SOD-like properties. The authors demonstrated that Fe-SAs/NC could protect cells from oxidative stress by removing H_2O_2 and O_2^- with minimal cytotoxicity [120].

Lu et al. designed a Fe-N/C SAN which possessed diverse enzyme mimic activities, including POD-mimic, CAT-mimic, OXD-mimic, and GPx-mimic activities. The Fe-N/C SAN powerfully scavenged intracellular ROS in HeLa cells because of the CAT-mimic and GPx-mimic activities [121].

Brain trauma always induces the generation of ROS, which subsequently leads to a complex cascade of biochemical responses and even permanent damage. Yan and fellows developed single-atom Pt/CeO_2 as a bandage for non-invasive treatment of traumatic brain injury (TBI) [122]. In comparison with CeO_2 clusters, Pt/CeO_2 displayed a significant higher ROS and RNS scavenging activity, and higher multiple enzyme catalytic activity. *In vitro* results showed Pt/CeO_2 remarkably downregulated the levels of inflammatory cytokines. *In vivo* experiments demonstrated the single-atom Pt/CeO_2 based bandage could significantly reduce the size and area of wound, remove the ROS near injured tissues, and recover the SOD and MMP-9 levels, resulting in a reduction in overall neuroinflammation (Fig. 9).

6 Conclusions

Benefiting from low costs, desirable stability, and modification versatility, nanozymes successfully overcome the disadvantages of natural enzymes and show great potential in biomedical applications. Nevertheless, the catalytic activity of nanozymes is

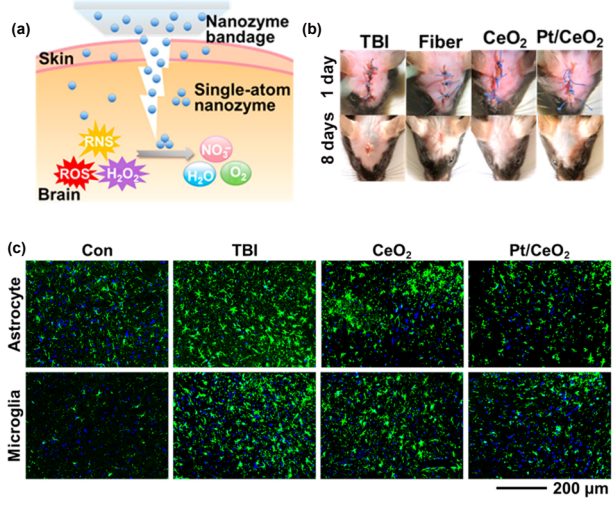

Figure 9 Application of single-atom nanozyme in noninvasive treatment of brain trauma. (a) Noninvasive TBI treatment through Pt/CeO_2. (b) Representative photos of wound healing over time. (c) Recruitment of astrocyte and microglia was obviously reduced in Pt/CeO_2 group, suggesting a decrease in neuroinflammation. Reproduced with permission from Ref. [122], © American Chemical Society 2019.

not ideal due to the low active site density of nanozymes and the fact that only the surface atomic layer participates in the catalytic reaction. Moreover, the unsatisfactory selectivity of nanozymes limits its practical applications [123]. The emergence of SANs has been identified as a breakthrough of nanozyme due to their multiple merits like higher selectivity and remarkable catalytic activity. By summarizing the biomedical applications of SANs, we firmly believe that SANs have a broad range of applications in the future. However, SANs are in the early stage of development, and still face some challenges.

(1) Biosafety

When used *in vivo*, the biosafety of materials, especially long-term biosafety, is a primary concern. Presently, most reported SANs showed good biocompatibility and low toxicology. However, SANs have only been reported for over a decade and their long-term biosafety has not been well explored. The large-sized SANs may prolong blood circulation time and accumulate in the body, resulting in potential cytotoxicity, while the small-sized SANs may cross the blood-brain barrier and produce some adverse effects. Furthermore, the metabolic characteristics and cytotoxicity of SANs can be affected by many factors, such as light, temperature, pH, and solvent. Therefore, it is required to systematically investigate their pharmacokinetics, potential cytotoxicity, and immunogenicity.

(2) Therapeutic efficacy

All natural enzymes in body are tightly and precisely regulated by the complex biological microenvironments. The complicated microenvironment and immune systems may reduce the efficacy of SANs. SANs need to be delicately designed to enhance the specific targeting ability for improving the therapeutic specificity and efficacy.

(3) Detailed catalytic mechanisms

Although catalytic mechanism can be calculated by density functional theory (DFT) calculations, it is difficult for DFT theoretical calculations to verify catalytic mechanisms under real conditions, especially in complex biological experiments. It is of great significance to develop more atomic resolution *in situ* characterization tools to clarify the catalytic mechanism.

(4) The scope of biomedical applications

Current SANs that mimic enzymes are mainly exhibited POD or OXD activity to generate ROS. There have been few reports of SANs mimicking other natural enzymes, which are insufficient to meet various clinical needs. The applications of SANs in the biomedical field are mainly concentrated in cancer treatments, antibacterial therapy, antioxidant therapy, and biosensing. However, biomedical applications in other fields such as drug delivery and tissue engineering should be explored. It is highly imperative to develop SANs with new enzyme-like properties to broaden their practical applications.

References

[1] Rehm, F. B. H.; Chen, S. X.; Rehm, B. H. A. Enzyme engineering for *in situ* immobilization. *Molecules* **2016**, *21*, 1370.

[2] Katsimpouras, C.; Stephanopoulos, G. Enzymes in biotechnology: Critical platform technologies for bioprocess development. *Curr. Opin. Biotechnol.* **2021**, *69*, 91–102.

[3] Sánchez-deAlcázar, D.; Liutkus, M.; Cortajarena, A. L. Immobilization of enzymes in protein films. In *Immobilization of Enzymes and Cells: Methods and Protocols*, 4th ed.; Guisan, J. M.; Bolivar, J. M.; López-Gallego, F.; Rocha-Martín, J., Eds.; Springer: New York, 2020; pp 211–226.

[4] Hao, J. C.; Zhuang, Z. C.; Cao, K. C.; Gao, G. H.; Wang, C.; Lai, F. L.; Lu, S. L.; Ma, P. M.; Dong, W. F.; Liu, T. X. et al. Unraveling the electronegativity-dominated intermediate adsorption on high-entropy alloy electrocatalysts. *Nat. Commun.* **2022**, *13*, 2662.

[5] Liu, Z. H.; Du, Y.; Zhang, P. F.; Zhuang, Z. C.; Wang, D. S. Bringing catalytic order out of chaos with nitrogen-doped ordered mesoporous carbon. *Matter* **2021**, *4*, 3161–3194.

[6] Zhuang, Z. C.; Huang, J. Z.; Li, Y.; Zhou, L.; Mai, L. Q. The holy grail in platinum-free electrocatalytic hydrogen evolution: Molybdenum-based catalysts and recent advances. *ChemElectroChem.* **2019**, *6*, 3570–3589.

[7] Zhuang, Z. C.; Li, Y.; Huang, J. Z.; Li, Z. L.; Zhao, K. N.; Zhao, Y. L.; Xu, L.; Zhou, L.; Moskaleva, L. V.; Mai, L. Q. *Sisyphus* effects in hydrogen electrochemistry on metal silicides enabled by silicene subunit edge. *Sci. Bull.* **2019**, *64*, 617–624.

[8] Zandieh, M.; Liu, J. W. Nanozyme catalytic turnover and self-limited reactions. *ACS Nano* **2021**, *15*, 15645–15655.

[9] Jiang, D. W.; Ni, D. L.; Rosenkrans, Z. T.; Huang, P.; Yan, X. Y.; Cai, W. B. Nanozyme: New horizons for responsive biomedical applications. *Chem. Soc. Rev.* **2019**, *48*, 3683–3704.

[10] Manea, F.; Houillon, F. B.; Pasquato, L.; Scrimin, P. Nanozymes: Gold-nanoparticle-based transphosphorylation catalysts. *Angew. Chem., Int. Ed.* **2004**, *43*, 6165–6169.

[11] Gao, L. Z.; Zhuang, J.; Nie, L.; Zhang, J. B.; Zhang, Y.; Gu, N.; Wang, T. H.; Feng, J.; Yang, D. L.; Perrett, S. et al. Intrinsic peroxidase-like activity of ferromagnetic nanoparticles. *Nat. Nanotechnol.* **2007**, *2*, 577–583.

[12] Zhang, Y. N.; Jin, Y. L.; Cui, H. X.; Yan, X. Y.; Fan, K. L. Nanozyme-based catalytic theranostics. *RSC Adv.* **2020**, *10*, 10–20.

[13] Mahmudunnabi, R. G.; Farhana, F. Z.; Kashaninejad, N.; Firoz, S. H.; Shim, Y. B.; Shiddiky, M. J. A. Nanozyme-based electrochemical biosensors for disease biomarker detection. *Analyst* **2020**, *145*, 4398–4420.

[14] Wang, Q.; Jiang, J.; Gao, L. Z. Nanozyme-based medicine for enzymatic therapy: Progress and challenges. *Biomed. Mater.* **2021**, *16*, 042002.

[15] Qiao, B. T.; Wang, A. Q.; Yang, X. F.; Allard, L. F.; Jiang, Z.; Cui, Y. T.; Liu, J. Y.; Li, J.; Zhang, T. Single-atom catalysis of CO oxidation using Pt_1/FeO_x. *Nat. Chem.* **2011**, *3*, 634–641.

[16] Jiao, L.; Yan, H. Y.; Wu, Y.; Gu, W. L.; Zhu, C. Z.; Du, D.; Lin, Y. H. When nanozymes meet single-atom catalysis. *Angew. Chem., Int. Ed.* **2020**, *59*, 2565–2576.

[17] Wang, S. Y.; Li, J. Q.; Li, Q.; Bai, X. W.; Wang, J. L. Metal single-atom coordinated graphitic carbon nitride as an efficient catalyst for CO oxidation. *Nanoscale* **2020**, *12*, 364–371.

[18] Wang, Y. Y.; Wu, D. H.; Lv, P.; He, B. L.; Li, X.; Ma, D. W.; Jia, Y. Theoretical insights into the electroreduction of nitrate to ammonia on graphene-based single-atom catalysts. *Nanoscale* **2022**, *14*, 10862–10872.

[19] Chen, Y. J.; Wang, P. X.; Hao, H. G.; Hong, J. J.; Li, H. J.; Ji, S. F.; Li, A.; Gao, R.; Dong, J. C.; Han, X. D. et al. Thermal atomization of platinum nanoparticles into single atoms: An effective strategy for engineering high-performance nanozymes. *J. Am. Chem. Soc.* **2021**, *143*, 18643–18651.

[20] Ji, S. F.; Jiang, B.; Hao, H. G.; Chen, Y. J.; Dong, J. C.; Mao, Y.; Zhang, Z. D.; Gao, R.; Chen, W. X.; Zhang, R. F. et al. Matching the kinetics of natural enzymes with a single-atom iron nanozyme. *Nat. Catal.* **2021**, *4*, 407–417.

[21] Li, R. Z.; Wang, D. S. Understanding the structure–performance relationship of active sites at atomic scale. *Nano Res.* **2022**, *15*, 6888–6923.

[22] Zheng, X. B.; Li, B. B.; Wang, Q. S.; Wang, D. S.; Li, Y. D. Emerging low-nuclearity supported metal catalysts with atomic level precision for efficient heterogeneous catalysis. *Nano Res.* **2022**, *15*, 7806–7839.

[23] Wang, Y.; Zheng, M.; Li, Y. R.; Ye, C. L.; Chen, J.; Ye, J. Y.; Zhang, Q. H.; Li, J.; Zhou, Z. Y.; Fu, X. Z. et al. p-d orbital hybridization induced by a monodispersed Ga site on a Pt_3Mn nanocatalyst boosts ethanol electrooxidation. *Angew. Chem., Int. Ed.* **2022**, *61*, e202115735.

[24] Chen, S. H.; Li, W. H.; Jiang, W. J.; Yang, J. R.; Zhu, J. X.; Wang, L. Q.; Ou, H. H.; Zhuang, Z. C.; Chen, M. Z.; Sun, X. H. et al. MOF encapsulating n-heterocyclic carbene-ligated copper single-atom site catalyst towards efficient methane electrosynthesis.

Angew. Chem., Int. Ed. **2022**, *61*, e202114450.
[25] Xiong, Y.; Sun, W. M.; Han, Y. H.; Xin, P. Y.; Zheng, X. S.; Yan, W. S.; Dong, J. C.; Zhang, J.; Wang, D. S.; Li, Y. D. Cobalt single atom site catalysts with ultrahigh metal loading for enhanced aerobic oxidation of ethylbenzene. *Nano Res.* **2021**, *14*, 2418–2423.
[26] Yang, J. R.; Li, W. H.; Xu, K. N.; Tan, S. D.; Wang, D. S.; Li, Y. D. Regulating the tip effect on single-atom and cluster catalysts: Forming reversible oxygen species with high efficiency in chlorine evolution reaction. *Angew. Chem., Int. Ed.* **2022**, *61*, e202200366.
[27] Zhang, E. H.; Tao, L.; An, J. K.; Zhang, J. W.; Meng, L. Z.; Zheng, X. B.; Wang, Y.; Li, N.; Du, S. X.; Zhang, J. T. et al. Engineering the local atomic environments of indium single-atom catalysts for efficient electrochemical production of hydrogen peroxide. *Angew. Chem., Int. Ed.* **2022**, *61*, e202117347.
[28] Yang, J. R.; Li, W. H.; Tan, S. D.; Xu, K. N.; Wang, Y.; Wang, D. S.; Li, Y. D. The electronic metal–support interaction directing the design of single atomic site catalysts: Achieving high efficiency towards hydrogen evolution. *Angew. Chem., Int. Ed.* **2021**, *60*, 19085–19091.
[29] Han, A. L.; Wang, X. J.; Tang, K.; Zhang, Z. D.; Ye, C. L.; Kong, K. J.; Hu, H. B.; Zheng, L. R.; Jiang, P.; Zhao, C. X. et al. An adjacent atomic platinum site enables single-atom iron with high oxygen reduction reaction performance. *Angew. Chem., Int. Ed.* **2021**, *60*, 19262–19271.
[30] Chen. Y. J.; Gao, R.; Ji, S. F.; Li, H. J.; Tang, K.; Jiang, P.; Hu, H. B.; Zhang, Z. D.; Hao, H. G.; Qu, Q. Y. et al. Atomic-level modulation of electronic density at cobalt single-atom sites derived from metal-organic frameworks: Enhanced oxygen reduction performance. *Angew. Chem., Int. Ed.* **2021**, *60*, 3212–3221.
[31] Zou, L. L.; Wei, Y. S.; Hou, C. C.; Li, C. X.; Xu Q. Single-Atom Catalysts Derived from Metal-Organic Frameworks for Electrochemical Applications. *Small* **2021**, *17*, e2004809.
[32] Zhu, P.; Xiong, X.; Wang, D. S. Regulations of active moiety in single atom catalysts for electrochemical hydrogen evolution reaction. *Nano Res.* **2022**, *15*, 5792–5815.
[33] Luo, S.; Gao, J. Q.; Chen, Y.; Ouyang, H.; Wang, L.; Fu, Z. F. Water dispersible cobalt single-atom catalysts with efficient chemiluminescence enhancement for sensitive bioassay. *Talanta* **2022**, *250*, 123732.
[34] Zhuang, Z. C.; Li, Y. H.; Yu, R. H.; Xia, L. X.; Yang, J. R.; Lang, Z. Q.; Zhu, J. X.; Huang, J. Z.; Wang, J. O.; Wang, Y. et al. Reversely trapping atoms from a perovskite surface for high-performance and durable fuel cell cathodes. *Nat. Catal.* **2022**, *5*, 300–310.
[35] Zhuang, Z. C.; Li, Y.; Li, Y. H.; Huang, J. Z.; Wei, B.; Sun, R.; Ren, Y. J.; Ding, J.; Zhu, J. X.; Lang, Z. Q. et al. Atomically dispersed nonmagnetic electron traps improve oxygen reduction activity of perovskite oxides. *Energy Environ. Sci.* **2021**, *14*, 1016–1028.
[36] Wang, Z. H.; Wu, F. G. Emerging single-atom catalysts/nanozymes for catalytic biomedical applications. *Adv. Healthc. Mater.* **2022**, *11*, e2101682.
[37] Mao, Y.; Gao, S. J.; Yao, L. L.; Wang, L.; Qu, H.; Wu, Y. E.; Chen, Y.; Zheng, L. Single-atom nanozyme enabled fast and highly sensitive colorimetric detection of Cr(VI). *J. Hazard. Mater.* **2021**, *408*, 124898.
[38] Pei, J. H.; Zhao, R. L.; Mu, X. Y.; Wang, J. Y.; Liu, C. L.; Zhang, X. D. Single-atom nanozymes for biological applications. *Biomater. Sci.* **2020**, *8*, 6428–6441.
[39] Shen, L. H.; Ye, D. X.; Zhao, H. B.; Zhang, J. J. Perspectives for single-atom nanozymes: Advanced synthesis, functional mechanisms, and biomedical applications. *Anal. Chem.* **2021**, *93*, 1221–1231.
[40] Shi, Q. L.; Yu, T. R.; Wu, R. F.; Liu, J. Metal–support interactions of single-atom catalysts for biomedical applications. *ACS Appl. Mater. Interfaces* **2021**, *13*, 60815–60836.
[41] Mancuso, G.; Midiri, A.; Gerace, E.; Biondo, C. Bacterial antibiotic resistance: The most critical pathogens. *Pathogens* **2021**, *10*, 1310.
[42] Drekonja, D. M.; Johnson, J. R. Identifying antibiotic-resistant infections. *Health Aff.* **2018**, *37*, 1014–1015.
[43] Li, Y. Y.; Zhu, W. X.; Li, J. S.; Chu, H. T. Research progress in nanozyme-based composite materials for fighting against bacteria and biofilms. *Colloids Surf. B Biointerfaces* **2021**, *198*, 111465.
[44] Zhou, C. Y.; Wang, Q.; Jiang, J.; Gao, L. Z. Nanozybiotics: Nanozyme-based antibacterials against bacterial resistance. *Antibiotics (Basel)* **2022**, *11*, 390.
[45] Wang, Q.; Jiang, J.; Gao, L. Z. Catalytic antimicrobial therapy using nanozymes. *Wiley Interdiscip. Rev. Nanomed. Nanobiotechnol.* **2022**, *14*, e1769.
[46] Feng, X. B.; Lei, J.; Ma, L.; Ouyang, Q. L.; Zeng, Y. X.; Liang, H.; Lei, C. C.; Li, G. C.; Tan, L.; Liu, X. M. et al. Ultrasonic interfacial engineering of MoS_2-modified Zn single-atom catalysts for efficient osteomyelitis sonodynamic ion therapy. *Small* **2022**, *18*, e2105775.
[47] Yu, Y.; Tan, L.; Li, Z. Y.; Liu, X. M.; Zheng, Y. F.; Feng, X. B.; Liang, Y. Q.; Cui, Z. D.; Zhu, S. L.; Wu, S. L. Single-atom catalysis for efficient sonodynamic therapy of methicillin-resistant *Staphylococcus aureus*-infected osteomyelitis. *ACS Nano* **2021**, *15*, 10628–10639.
[48] Wang, X. W.; Shi, Q. Q.; Zha, Z.; Zhu, D. D.; Zheng, L. R.; Shi, L. X.; Wei, X. W.; Lian, L.; Wu, K. L.; Cheng, L. Copper single-atom catalysts with photothermal performance and enhanced nanozyme activity for bacteria-infected wound therapy. *Bioact. Mater.* **2021**, *6*, 4389–4401.
[49] Xu, B. L.; Wang, H.; Wang, W. W.; Gao, L. Z.; Li, S. S.; Pan, X. T.; Wang, H. Y.; Yang, H. L.; Meng, X. Q.; Wu, Q. W. et al. A single-atom nanozyme for wound disinfection applications. *Angew. Chem., Int. Ed.* **2019**, *58*, 4911–4916.
[50] Huo, M. F.; Wang, L. Y.; Zhang, H. X.; Zhang, L. L.; Chen, Y.; Shi, J. L. Construction of single-iron-atom nanocatalysts for highly efficient catalytic antibiotics. *Small* **2019**, *15*, e1901834.
[51] Huang, L.; Chen, J. X.; Gan, L. F.; Wang, J.; Dong, S. J. Single-atom nanozymes. *Sci. Adv.* **2019**, *5*, eaav5490.
[52] Cao, F. F.; Zhang, L.; You, Y. W.; Zheng, L. R.; Ren, J. S.; Qu, X. G. An enzyme-mimicking single-atom catalyst as an efficient multiple reactive oxygen and nitrogen species scavenger for sepsis management. *Angew. Chem., Int. Ed.* **2020**, *59*, 5108–5115.
[53] Wang, D. J.; Zhang, B.; Ding, H.; Liu, D.; Xiang, J. Q.; Gao, X. J.; Chen, X. H.; Li, Z. J.; Yang, L.; Duan, H. X. et al. TiO_2 supported single Ag atoms nanozyme for elimination of SARS-CoV2. *Nano Today* **2021**, *40*, 101243.
[54] Wu, S. Z.; Wu, B. J.; Liu, Y. J.; Deng, S.; Lei, L.; Zhang, H. Mini review therapeutic strategies targeting for biofilm and bone infections. *Front. Microbiol.* **2022**, *13*, 936285.
[55] Meroni, G.; Tsikopoulos, A.; Tsikopoulos, K.; Allemanno, F.; Martino, P. A.; Soares Filipe, J. F. A journey into animal models of human osteomyelitis: A review. *Microorganisms* **2022**, *10*, 1135.
[56] Jari Litany, R. I.; Praseetha, P. K. Tiny tots for a big-league in wound repair: Tools for tissue regeneration by nanotechniques of today. *J. Control. Release* **2022**, *349*, 443–459.
[57] Liu, Y. H.; Xu, B. L.; Lu, M. Z.; Li, S. S.; Guo, J.; Chen, F. Z.; Xiong, X. L.; Yin, Z.; Liu, H. Y.; Zhou, D. S. Ultrasmall Fe-doped carbon dots nanozymes for photoenhanced antibacterial therapy and wound healing. *Bioact. Mater.* **2022**, *12*, 246–256.
[58] Dartiguelongue, J. B. Systemic inflammation and sepsis. Part I: Storm formation. *Arch. Argent. Pediatr.* **2020**, *118*, e527–e535.
[59] Wan Muhd Shukeri, W. F.; Mat Nor, M. B.; Md Ralib, A. Sepsis and its impact on outcomes in elderly patients admitted to a Malaysian intensive care unit. *Malays. J. Med. Sci.* **2022**, *29*, 145–150.
[60] Liu, T. T.; Tang, X. M.; Cui, Y.; Xiong, X.; Xu, Y. Y.; Hu, S. H.; Feng, S. Y.; Shao, L. J.; Ren, Y. Q.; Miao, H. J. et al. Fibroblast growth factor 19 improves LPS-induced lipid disorder and organ injury by regulating metabolomic characteristics in mice. *Oxid. Med. Cell. Longev.* **2022**, *2022*, 9673512.
[61] Shimizu, J.; Murao, A.; Nofi, C.; Wang, P.; Aziz, M. Extracellular CIRP promotes GPX4-mediated ferroptosis in sepsis. *Front. Immunol.* **2022**, *13*, 903859.
[62] Maya, S.; Kahn, J. G.; Lin, T. K.; Jacobs, L. M.; Schmidt, L. A.; Burrough, W. B.; Ghasemzadeh, R.; Mousli, L.; Allan, M.; Donovan, M. et al. Indirect COVID-19 health effects and potential mitigating interventions: Cost-effectiveness framework. *PLoS One*

2022, *17*, e0271523.
[63] Yao, M.; Han, W. X.; Feng, L.; Wei, Z. Z.; Liu, Y.; Zhang, H. R.; Zhang, S. S. pH-programmed responsive nanoplatform for synergistic cancer therapy based on single atom catalysts. *Eur. J. Med. Chem.* **2022**, *233*, 114236.
[64] Yang, J. C.; Yao, H. L.; Guo, Y. D.; Yang, B. W.; Shi, J. L. Enhancing tumor catalytic therapy by co-catalysis. *Angew. Chem., Int. Ed.* **2022**, *61*, e202200480.
[65] Cao, F. F.; Sang, Y. J.; Liu, C. Y.; Bai, F. Q.; Zheng, L. R.; Ren, J. S.; Qu, X. G. Self-adaptive single-atom catalyst boosting selective ferroptosis in tumor cells. *ACS Nano* **2022**, *16*, 855–868.
[66] Lu, X. Y.; Gao, S. S.; Lin, H.; Shi, J. L. Single-atom catalysts for nanocatalytic tumor therapy. *Small* **2021**, *17*, e2004467.
[67] Wang, L.; Qu, X. Z.; Zhao, Y. X.; Weng, Y. Z. W.; Waterhouse, G. I. N.; Yan, H.; Guan, S. Y.; Zhou, S. Y. Exploiting single atom iron centers in a porphyrin-like MOF for efficient cancer phototherapy. *ACS Appl. Mater. Interfaces* **2019**, *11*, 35228–35237.
[68] Huo, M. F.; Wang, L. Y.; Wang, Y. W.; Chen, Y.; Shi, J. L. Nanocatalytic tumor therapy by single-atom catalysts. *ACS Nano* **2019**, *13*, 2643–2653.
[69] Fan, Y.; Liu, S. G.; Yi, Y.; Rong, H. P.; Zhang, J. T. Catalytic nanomaterials toward atomic levels for biomedical applications: From metal clusters to single-atom catalysts. *ACS Nano* **2021**, *15*, 2005–2037.
[70] Xu, Q. Q.; Zhang, Y. T.; Yang, Z. L.; Jiang, G. H.; Lv, M. Z.; Wang, H.; Liu, C. H.; Xie, J. N.; Wang, C. Y.; Guo, K. et al. Tumor microenvironment-activated single-atom platinum nanozyme with H_2O_2 self-supplement and O_2-evolving for tumor-specific cascade catalysis chemodynamic and chemoradiotherapy. *Theranostics* **2022**, *12*, 5155–5171.
[71] Li, B.; Guo, L. B.; Chen, M. J.; Guo, Y. Y.; Ge, L. L.; Kwok, H. F. Single-atom Pt-anchored $Zn_{0.5}Cd_{0.5}S$ boosted photoelectrochemical immunoassay of prostate-specific antigen. *Biosens. Bioelectron.* **2022**, *202*, 114006.
[72] Chen, Y. F.; Jiao, L.; Yan, H. Y.; Xu, W. Q.; Wu, Y.; Zheng, L. R.; Gu, W. L.; Zhu, C. Z. Fe-N-C single-atom catalyst coupling with Pt clusters boosts peroxidase-like activity for cascade-amplified colorimetric immunoassay. *Anal. Chem.* **2021**, *93*, 12353–12359.
[73] Wang, W. Y.; Zhu, Y.; Zhu, X. R.; Zhao, Y. F.; Xue, Z. G.; Xiong, C.; Wang, Z. Y.; Qu, Y. T.; Cheng, J. J.; Chen, M. et al. Biocompatible ruthenium single-atom catalyst for cascade enzyme-mimicking therapy. *ACS Appl. Mater. Interfaces* **2021**, *13*, 45269–45278.
[74] Wang, D. D.; Wu, H. H.; Phua, S. Z. F.; Yang, G. B.; Qi Lim, W.; Gu, L.; Qian, C.; Wang, H. B.; Guo, Z.; Chen, H. Z. et al. Self-assembled single-atom nanozyme for enhanced photodynamic therapy treatment of tumor. *Nat. Commun.* **2020**, *11*, 357.
[75] Xu, B. L.; Li, S. S.; Zheng, L. R.; Liu, Y. H.; Han, A. L.; Zhang, J.; Huang, Z. J.; Xie, H. J.; Fan, K. L.; Gao, L. Z. et al. A bioinspired five-coordinated single-atom iron nanozyme for tumor catalytic therapy. *Adv. Mater.* **2022**, *34*, e2107088.
[76] Zhu, Y.; Wang, W. Y.; Cheng, J. J.; Qu, Y. T.; Dai, Y.; Liu, M. M.; Yu, J. N.; Wang, C. M.; Wang, H. J.; Wang, S. C. et al. Stimuli-responsive manganese single-atom nanozyme for tumor therapy via integrated cascade reactions. *Angew. Chem., Int. Ed.* **2021**, *60*, 9480–9488.
[77] Chang, M. Y.; Hou, Z. Y.; Wang, M.; Yang, C. Z.; Wang, R. F.; Li, F.; Liu, D. L.; Peng, T. L.; Li, C. X.; Lin, J. Single-atom Pd nanozyme for ferroptosis-boosted mild-temperature photothermal therapy. *Angew. Chem., Int. Ed.* **2021**, *60*, 12971–12979.
[78] Qi, P. Y.; Zhang, J. Y.; Bao, Z. R.; Liao, Y. P.; Liu, Z. M.; Wang, J. K. A platelet-mimicking single-atom nanozyme for mitochondrial damage-mediated mild-temperature photothermal therapy. *ACS Appl. Mater. Interfaces* **2022**, *14*, 19081–19090.
[79] Su, Y. T.; Wu, F.; Song, Q. X.; Wu, M. J.; Mohammadniaei, M.; Zhang, T. W.; Liu, B. L.; Wu, S. S.; Zhang, M.; Li, A. et al. Dual enzyme-mimic nanozyme based on single-atom construction strategy for photothermal-augmented nanocatalytic therapy in the second near-infrared biowindow. *Biomaterials* **2022**, *281*, 121325.
[80] Liu, Y.; Yao, M.; Han, W. X.; Zhang, H. R.; Zhang, S. S. Construction of a single-atom nanozyme for enhanced chemodynamic therapy and chemotherapy. *Chem.—Eur. J.* **2021**, *27*, 13418–13425.
[81] Feng, N.; Li, Q.; Bai, Q.; Xu, S. C.; Shi, J. X.; Liu, B. J.; Guo, J. C. Development of an Au-anchored Fe single-atom nanozyme for biocatalysis and enhanced tumor photothermal therapy. *J. Colloid Interface Sci.* **2022**, *618*, 68–77.
[82] Wang, L. Y.; Yang, Q. H.; Huo, M. F.; Lu, D.; Gao, Y. S.; Chen, Y.; Xu, H. X. Engineering single-atomic iron-catalyst-integrated 3D-printed bioscaffolds for osteosarcoma destruction with antibacterial and bone defect regeneration bioactivity. *Adv. Mater.* **2021**, *33*, e2100150.
[83] Gong, N. Q.; Ma, X. W.; Ye, X. X.; Zhou, Q. F.; Chen, X. A.; Tan, X. L.; Yao, S. K.; Huo, S. D.; Zhang, T. B.; Chen, S. Z. et al. Carbon-dot-supported atomically dispersed gold as a mitochondrial oxidative stress amplifier for cancer treatment. *Nat Nanotechnol.* **2019**, *14*, 379–387.
[84] Zhang, Z. X.; Zhanghuang, C.; Wang, J. K.; Tian, X. M.; Wu, X.; Li, M. X.; Mi, T.; Liu, J. Y.; Jin, L. M.; Li, M. J. et al. Development and validation of nomograms to predict cancer-specific survival and overall survival in elderly patients with prostate cancer: A population-based study. *Front. Oncol.* **2022**, *12*, 918780.
[85] Israël, B.; Hannink, G.; Barentsz, J. O.; van der Leest, M. M. G. Implications of the European association of urology recommended risk assessment algorithm for early prostate cancer detection. *Eur. Urol. Open Sci.* **2022**, *43*, 1–4.
[86] Vargovčák, M.; Dorko, E.; Rimárová, K.; Knap, V. Prostate cancer screening—Is it time to change approach? *Cent. Eur. J. Public Health* **2022**, *30*, S11–S15.
[87] Cao, W.; Chen, H. D.; Yu, Y. W.; Li, N.; Chen, W. Q. Changing profiles of cancer burden worldwide and in China: A secondary analysis of the global cancer statistics 2020. *Chin. Med. J.* **2021**, *134*, 783–791.
[88] Yang, L.; Du, X.; Qin, Y. R.; Wang, X. Y.; Zhang, L. F.; Chen, Z. M.; Wang, Z. J.; Yang, X.; Lei, M.; Zhu, Y. Q. Biomimetic multifunctional nanozymes enhanced radiosensitization for breast cancer via an X-ray triggered cascade reaction. *J. Mater. Chem. B* **2022**, *10*, 3667–3680.
[89] Darabi, F.; Saidijam, M.; Nouri, F.; Mahjub, R.; Soleimani, M. Anti-CD44 and EGFR dual-targeted solid lipid nanoparticles for delivery of doxorubicin to triple-negative breast cancer cell line: Preparation, statistical optimization, and *in vitro* characterization. *Biomed. Res. Int.* **2022**, *2022*, 6253978.
[90] Zhang, Y.; Ding, X.; Xie, F.; Gao, M. J.; Qiu, J. L.; Wang, Z. W.; Qing, L.; Yan, J. Q.; Peng, N.; Li, Y. Y. et al. Targeted recruitment and degradation of estrogen receptor α by photothermal polydopamine nanoparticles for breast tumor ablation. *Adv. Healthc. Mater.*, in press, https://doi.org/10.1002/adhm.202200960.
[91] Alamdari, S. G.; Amini, M.; Jalilzadeh, N.; Baradaran, B.; Mohammadzadeh, R.; Mokhtarzadeh, A.; Oroojalian, F. Recent advances in nanoparticle-based photothermal therapy for breast cancer. *J. Control. Release* **2022**, *349*, 269–303.
[92] Archer, J. M.; Truong, M. T.; Shroff, G. S.; Godoy, M. C. B.; Marom, E. M. Imaging of lung cancer staging. *Semin. Respir. Crit. Care Med.*, in press, https://doi.org/10.1055/s-0042-1753476.
[93] Zhou, X. T.; You, M.; Wang, F. H.; Wang, Z. Z.; Gao, X. F.; Jing, C.; Liu, J. M.; Guo, M. Y.; Li, J. Y.; Luo, A. P. et al. Multifunctional graphdiyne-cerium oxide nanozymes facilitate MicroRNA delivery and attenuate tumor hypoxia for highly efficient radiotherapy of esophageal cancer. *Adv. Mater.* **2021**, *33*, e2100556.
[94] Wang, Y. F.; Zhang, W. H.; Sun, J. W.; Wang, L. D.; Song, X.; Zhao, X. K. Survival risk prediction of esophageal squamous cell carcinoma based on BES-LSSVM. *Comput. Intell. Neurosci.* **2022**, *2022*, 3895590.
[95] Xie, X. L.; Wang, D. P.; Guo, C. X.; Liu, Y. H.; Rao, Q. H.; Lou, F. M.; Li, Q. N.; Dong, Y. Q.; Li, Q. F.; Yang, H. B. et al. Single-atom ruthenium biomimetic enzyme for simultaneous electrochemical detection of dopamine and uric acid. *Anal. Chem.*

2021, *93*, 4916–4923.

[96] Feng, M.; Zhang, Q.; Chen, X. F.; Deng, D.; Xie, X. Y.; Yang, X. P. Controllable synthesis of boron-doped Zn-N-C single-atom nanozymes for the ultrasensitive colorimetric detection of p-phenylenediamine. *Biosens. Bioelectron.* **2022**, *210*, 114294.

[97] Luo, X.; Luo, Z.; Wei, X. Q.; Jiao, L.; Fang, Q.; Wang, H. J.; Wang, J. H.; Gu, W. L.; Hu, L. Y.; Zhu, C. Z. Iridium single-atomic site catalysts with superior oxygen reduction reaction activity for sensitive monitoring of organophosphorus pesticides. *Anal. Chem.* **2022**, *94*, 1390–1396.

[98] Xu, W. Q.; Song, W. Y.; Kang, Y. K.; Jiao, L.; Wu, Y.; Chen, Y. F.; Cai, X. L.; Zheng, L. R.; Gu, W. L.; Zhu, C. Z. Axial ligand-engineered single-atom catalysts with boosted enzyme-like activity for sensitive immunoassay. *Anal. Chem.* **2021**, *93*, 12758–12766.

[99] Bushira, F. A.; Kitte, S. A.; Xu, C.; Li, H. J.; Zheng, L.; Wang, P.; Jin, Y. D. Two-dimensional-plasmon-boosted iron single-atom electrochemiluminescence for the ultrasensitive detection of dopamine, hemin, and mercury. *Anal. Chem.* **2021**, *93*, 9949–9957.

[100] Lyu, Z. Y.; Ding, S. C.; Wang, M. Y.; Pan, X. Q.; Feng, Z. X.; Tian, H. Y.; Zhu, C. Z.; Du, D.; Lin, Y. H. Iron-imprinted single-atomic site catalyst-based nanoprobe for detection of hydrogen peroxide in living cells. *Nanomicro. Lett.* **2021**, *13*, 146.

[101] Jiao, L.; Xu, W. Q.; Wu, Y.; Yan, H. Y.; Gu, W. L.; Du, D.; Lin, Y. H.; Zhu, C. Z. Single-atom catalysts boost signal amplification for biosensing. *Chem. Soc. Rev.* **2021**, *50*, 750–765.

[102] Wu, W. W.; Huang, L.; Zhu, X. Y.; Chen, J. X.; Chao, D. Y.; Li, M. H.; Wu, S. L.; Dong, S. J. Reversible inhibition of the oxidase-like activity of Fe single-atom nanozymes for drug detection. *Chem. Sci.* **2022**, *13*, 4566–4572.

[103] Song, G. C.; Li, J. C.; Majid, Z.; Xu, W. T.; He, X. Y.; Yao, Z. Y.; Luo, Y. B.; Huang, K. L.; Cheng, N. Phosphatase-like activity of single-atom Ce-N-C nanozyme for rapid detection of Al^{3+}. *Food Chem.* **2022**, *390*, 133127.

[104] Wu, Y.; Wu, J. B.; Jiao, L.; Xu, W. Q.; Wang, H. J.; Wei, X. Q.; Gu, W. L.; Ren, G. X.; Zhang, N.; Zhang, Q. H. et al. Cascade reaction system integrating single-atom nanozymes with abundant Cu sites for enhanced biosensing. *Anal. Chem.* **2020**, *92*, 3373–3379.

[105] Wu, Y.; Jiao, L.; Luo, X.; Xu, W. Q.; Wei, X. Q.; Wang, H. J.; Yan, H. Y.; Gu, W. L.; Xu, B. Z.; Du, D. et al. Oxidase-like Fe-N-C single-atom nanozymes for the detection of acetylcholinesterase activity. *Small* **2019**, *15*, e1903108.

[106] Qin, Y.; Wen, J.; Wang, X. S.; Jiao, L.; Wei, X. Q.; Wang, H. J.; Li, J. L.; Liu, M. W.; Zheng, L. R.; Hu, L. Y. et al. Iron single-atom catalysts boost photoelectrochemical detection by integrating interfacial oxygen reduction and enzyme-mimicking activity. *ACS Nano* **2022**, *16*, 2997–3007.

[107] Niu, X. H.; Shi, Q. R.; Zhu, W. L.; Liu, D.; Tian, H. Y.; Fu, S. F.; Cheng, N.; Li, S. Q.; Smith, J. N.; Du, D. et al. Unprecedented peroxidase-mimicking activity of single-atom nanozyme with atomically dispersed Fe-N_x moieties hosted by MOF derived porous carbon. *Biosens. Bioelectron.* **2019**, *142*, 111495.

[108] Xie, X. L.; Wang, Y. F.; Zhou, X. B.; Chen, J. Y.; Wang, M. K.; Su, X. G. Fe-N-C single-atom nanozymes with peroxidase-like activity for the detection of alkaline phosphatase. *Analyst* **2021**, *146*, 896–903.

[109] Chen, Q. M.; Li, S. Q.; Liu, Y.; Zhang, X. D.; Tang, Y.; Chai, H. X.; Huang, Y. M. Size-controllable Fe-N/C single-atom nanozyme with exceptional oxidase-like activity for sensitive detection of alkaline phosphatase. *Sens. Actuators B:Chem.* **2020**, *305*, 127511.

[110] Cheng, N.; Li, J. C.; Liu, D.; Lin, Y. H.; Du, D. Single-atom nanozyme based on nanoengineered Fe-N-C catalyst with superior peroxidase-like activity for ultrasensitive bioassays. *Small* **2019**, *15*, e1901485.

[111] Hou, H. F.; Mao, J. J.; Han, Y. H.; Wu, F.; Zhang, M. N.; Wang, D. S.; Mao, L. Q.; Li, Y. D. Single-atom electrocatalysis: A new approach to *in vivo* electrochemical biosensing. *Sci. China Chem.* **2019**, *62*, 1720–1724.

[112] Chen, M.; Zhou, H.; Liu, X. K.; Yuan, T. W.; Wang, W. Y.; Zhao, C.; Zhao, Y. F.; Zhou, F. Y.; Wang, X.; Xue, Z. G. et al. Single iron site nanozyme for ultrasensitive glucose detection. *Small* **2020**, *16*, e2002343.

[113] Wang, Y.; Zhang, Z. W.; Jia, G. R.; Zheng, L. R.; Zhao, J. X.; Cui, X. Q. Elucidating the mechanism of the structure-dependent enzymatic activity of Fe-N/C oxidase mimics. *Chem. Commun. (Camb.)* **2019**, *55*, 5271–5274.

[114] Liu, Y.; Yan, J. H.; Huang, Y.; Sun, Z. H.; Zhang, H. J.; Fu, L. H. Y.; Li, X. W.; Jin, Y. R. Single-atom Fe-anchored nano-diamond with enhanced dual-enzyme mimicking performance for H_2O_2 and glutathione detection. *Front. Bioeng. Biotechnol.* **2022**, *9*, 790849.

[115] Jiao, L.; Xu, W. Q.; Yan, H. Y.; Wu, Y.; Liu, C. R.; Du, D.; Lin, Y. H.; Zhu, C. Z. Fe-N-C single-atom nanozymes for the intracellular hydrogen peroxide detection. *Anal. Chem.* **2019**, *91*, 11994–11999.

[116] Lai, X.; Shen, Y.; Gao, S. B.; Chen, Y. J.; Cui, Y. S.; Ning, D. X.; Ji, X. B.; Liu, Z. W.; Wang, L. G. The Mn-modified porphyrin metal-organic framework with enhanced oxidase-like activity for sensitively colorimetric detection of glutathione. *Biosens. Bioelectron.* **2022**, *213*, 114446.

[117] Li, D.; Tian, R.; Kang, S. Y.; Chu, X. Q.; Ge, D. H.; Chen, X. J. Fabrication of Ag nanoparticles coupled with ferrous disulfide biocatalyst as a peroxidase mimic for sensitive electrochemical and colorimetric dual-mode biosensing of H_2O_2. *Food Chem.* **2022**, *393*, 133386.

[118] Jiang, S.; Zhang, C. F.; Zou, T. Single-atom catalysts for biotherapy applications: A systematic review. *Nanomaterials (Basel)* **2020**, *10*, 2518.

[119] Xiang, H. J.; Feng, W.; Chen, Y. Single-atom catalysts in catalytic biomedicine. *Adv. Mater.* **2020**, *32*, e1905994.

[120] Ma, W. J.; Mao, J. J.; Yang, X. T.; Pan, C.; Chen, W. X.; Wang, M.; Yu, P.; Mao, L. Q.; Li, Y. D. A single-atom Fe-N_4 catalytic site mimicking bifunctional antioxidative enzymes for oxidative stress cytoprotection. *Chem. Commun. (Camb.)* **2019**, *55*, 159–162.

[121] Lu, M. J.; Wang, C.; Ding, Y. Q.; Peng, M. H.; Zhang, W.; Li, K.; Wei, W.; Lin, Y. Q. Fe-N/C single-atom catalysts exhibiting multienzyme activity and ROS scavenging ability in cells. *Chem. Commun. (Camb.)* **2019**, *55*, 14534–14537.

[122] Yan, R. J.; Sun, S.; Yang, J.; Long, W.; Wang, J. Y.; Mu, X. Y.; Li, Q. F.; Hao, W. T.; Zhang, S. F.; Liu, H. L. et al. Nanozyme-based bandage with single-atom catalysis for brain trauma. *ACS Nano* **2019**, *13*, 11552–11560.

[123] Wu, J. J. X.; Wang, X. Y.; Wang, Q.; Lou, Z. P.; Li, S. R.; Zhu, Y. Y.; Qin, L.; Wei, H. Nanomaterials with enzyme-like characteristics (nanozymes): Next-generation artificial enzymes(II). *Chem. Soc. Rev.* **2019**, *48*, 1004–1076.